International Journal of Biological Macromolecules 214 (2022) 128–139

Contents lists available at ScienceDirect

International Journal of Biological Macromolecules

journal homepage: www.elsevier.com/locate/ijbiomac

Effect of the structural features of biobased linear polyester plasticizers on the crystallization of polylactides

Maryam Safari [a,1], Nejib Kasmi [b,1,2], Carla Pisani [b], Vincent Berthé [b], Alejandro J. Müller [a,c,*], Youssef Habibi [b,*]

[a] POLYMAT and Department of Polymers and Advanced Materials: Physics, Chemistry and Technology, Faculty of Chemistry, University of the Basque Country UPV/EHU, Paseo Manuel de Lardizábal, 3, 20018 Donostia-San Sebastián, Spain
[b] Department of Materials Research and Technology (MRT), Luxembourg Institute of Science and Technology (LIST), 5 avenue des Hauts-Fourneaux, L-4362 Esch-sur-Alzette, Luxembourg
[c] IKERBASQUE, Basque Foundation for Science, Plaza Euskadi 5, 48009 Bilbao, Spain

ARTICLE INFO

Keywords:
Polylactide
Aliphatic polyester plasticizer
Spherulitic growth kinetics
Nucleation rate
Overall isothermal crystallization kinetics

ABSTRACT

This work presents, for the first time, a detailed report on how the nucleation and crystallization of polylactide (PLLA) are affected by biobased aliphatic polyesters plasticizers. Three biobased polyesters were synthesized via solvent-free two-stage melt polycondensation of adipic acid (AdA) with three different biobased aliphatic diols and used as plasticizers for poly (L-lactic acid) (PLLA). The molecular structure of the synthesized polyesters was proved using ^{1}H NMR, ^{13}C NMR and Fourier transform infrared (FTIR) spectroscopy. PLLA/AdA-based blends containing 10 wt% of the polyester plasticizers were studied by tensile tests, dynamic mechanical analysis (DMA), wide-angle x-ray scattering (WAXS), differential scanning calorimetry (DSC) and polarized light optical microscopy (PLOM). Adding the plasticizers to PLLA decreased T_g by up to 11 °C and significantly increased the elongation at break by about 8 times compared with neat PLLA. The addition of 10 wt% of any AdA-based plasticizer to PLLA increases the nucleation rate from the glassy state by around 50–110 % depending on the plasticizer. The overall crystallization rate from the glassy state was 2–3 times faster for the plasticized PLLAs than neat PLLA. These results are a consequence of the lower energy barrier for both nucleation and growth processes. The incorporation of AdA-based linear polyesters had an incremental impact on the crystal growth rate (or secondary nucleation) of PLLA spherulites from the melt and glassy states. In conclusion, the AdA-based aliphatic polyesters allowed to enhance PLLA crystallization rates and showed interesting potential for the formulation of fully biobased PLLA blends.

1. Introduction

Poly(lactic acid) PLA is currently considered as the leading biobased thermoplastic polymer. Increased volumes of production have been reported thanks to successful use in a wide range of applications. Indeed, PLA is degradable in industrial composting environment, biocompatible, biobased and presents advantageous mechanical properties. However, PLLA use in various moulding processes is hindered by its slow crystallization rate and its high brittleness compared to commodity polymers [1–3]. As a result, various affordable and practical blending strategies have been reported to efficiently improve its crystallization rate [4–6]:

- Addition of small nucleating agents (either inorganic or organic) to lower the surface free energy of nucleation, thus increasing crystallization temperatures upon cooling.
- Addition of plasticizers or miscible low T_g polymers to increase chain mobility and thus crystallization rates.

There is extensive research on PLLA plasticization. Focusing on molecular and oligomeric plasticizers, a variety of examples can be selected to try to summarize this vast literature. Some of the most well

* Corresponding authors.
E-mail addresses: alejandrojesus.muller@ehu.es (A.J. Müller), habibi_y@hotmail.fr (Y. Habibi).
[1] Equal contribution.
[2] Current address: KTH Royal Institute of Technology, Department of Fibre and Polymer Technology, Teknikringen 56-58, 10,044, Stockholm, Sweden.

https://doi.org/10.1016/j.ijbiomac.2022.06.056
Received 21 March 2022; Received in revised form 20 May 2022; Accepted 9 June 2022
Available online 11 June 2022

known plasticizers reported for PLA are triacetin [7] and poly(ethylene glycol) (PEG) [8–14]. Besides, citrate [7,15–17], laurate, and sebacate esters and fatty acids [8,18] have also been studied. The primary effect of these plasticizers is an increase in the crystallization rate, as shown by Kulinski and Piorkowska [14,19,20], it was also shown that oligomeric PEG could accelerate PLA spherulite growth rate [11]. However, while these blends show improved ductility their main drawbacks consist in significant T_g reductions [9,11] and the fact that low molecular weight plasticizers can leach out upon aging [21]. With this view, many bio-based oligomeric plasticizers have been reported, and the uses of such as poly(1,4-butylene azelate), poly(1,6-hexamethylene azelate) and poly (1,4-butylene succinate), have been patented as early as 1999 [22–24]. However, no detailed reports of the crystallization characteristics of those systems have been covered.

In this regard, Poly(1,4-butylene adipate) (AdA-1,4 BDO) [25], poly (2,3-butylene adipate) (AdA-2,3 BDO) [26] and poly(1,6-hexamethylene adipate) (AdA-1,6 HDO) [27] are also other relevant examples of fully biobased aliphatic polyesters with similar structural features. These thermoplastics can be prepared via solvent-free melt polycondensation by combining adipic acid (AdA) with different bio-based aliphatic diols: 1,4-butanediol, 2,3-butanediol and 1,6-hexanediol. Different synthetic approaches including catalytic conversion, enzymatic hydrolysis and fermentation of lignocellulosic biomass, mainly hydroxymethylfurfural (HMF), have been developed to give these renewable building blocks [28–31]. Although these biobased plasticizers materials have been extensively studied in PLA and reported in the literature for a long time, no detailed studies on crystallization have been reported yet.

This study evaluated the influence of the structure of renewable aliphatic AdA-based polyester plasticizers over the crystallization, crystallinity and thermo-mechanical properties of 90/10 w:w PLLA/plasticizer blends. Emphasis was put on plasticized PLLAs spherulitic growth kinetics and overall isothermal crystallization kinetics, aspects that had not been previously reported in the literature. Based on the results of crystallization from the melt (studied by PLOM) and glassy state (performed by DSC), the addition of 10 % of any ADA-based polyesters combined with PLLA caused an increase in the growth rate and overall crystallization rate of PLLA.

2. Experimental section

2.1. Materials

2,3-Butanediol (2,3 BDO, purum 98 %), 1,4-Butanediol (1,4 BDO, purum 99 %), 1,6-Hexandiol (1,6 HDO, purum 99 %) and adipic acid (AdA, purum 99. 5 %), reagents, tertrabutyl titanate (TBT) catalyst, were purchased from Sigma-Aldrich. All other solvents and materials used were of analytical grade. Poly(L-lactic acid) (PLLA) Ingeo 4032D was purchased from NatureWorks™ and used as received (M_n = 90,000 g/mol as determined by size-exclusion chromatography using PLA standards relative calibration curve, and 1.4 mol% of (D)-lactide content).

2.2. Polymer synthesis

As shown in Scheme 1 in Results and Discussion section, three fully biobased aliphatic polyesters were synthesized by the two-stage melt polycondensation procedure (esterification and polycondensation) as follows: a predetermined amount of AdA diacid and diol (1,4 BDO, 2,3 BDO, or 1,6 HDO) with the molar ratio of diacid: diol of 1:1.20 were introduced in presence of 400 ppm of TBT catalyst into the autoclave reactor equipped with a mechanical stirrer. At room temperature, the reagents mixture was evacuated several times and filled with nitrogen to remove the whole amount of oxygen, thus avoiding oxidation during the reaction. In the first esterification stage performed under nitrogen atmosphere, the reaction temperature was raised to 190 °C and the reaction was left to proceed at this temperature for 2.5 h for the polymer samples derived from 1,4 BDO and 2,3 BDO diols. For AdA-1,6 HDA polyester, the reactor temperature was gradually increased to 170 °C for 2 h, for an additional 1 h at 180 °C, and it was maintained finally at 190 °C for 0.5 h. The system pressure was then reduced slowly during polycondensation step to 10 mbar over a time of about 30 min to avoid excessive foaming and also to minimize the oligomers sublimation while the temperature was increased to the temperature range of 220–230 °C (for AdA-1,6 HDO polymer: 2.5 h at 220 °C, and for additional 0.5 h at 230 °C). Unlike, the second synthesis step lasted for 2.5 h for the other 2,3 BDO and 1,4 BDO-based polyesters, in which the temperature was raised to 220 °C for 1 h and for an additional 1.5 h at 230 °C. At last, after the polymerization of the target materials was completed, the melt was cooled to room temperature. The crude product was purified by dissolution in chloroform followed by precipitation in cold methanol. AdA-1,4 BDO, AdA-2,3 BDO and AdA-1,6 HDO are the abbreviations given to the prepared linear polyester based samples.

2.3. Polymer processing: melt blending and compression moulding

Prior to processing the PLLA and polyesters were dried at 50 °C under reduce pressure of 100 mbar in order to remove any residual organic solvent and humidity, thus preventing polyester hydrolysis. Polyesters plasticizers were melt-blended with PLLA at 10 wt% loading using a twin-screw 15 cm^3 micro-compounder (MC150, Xplore) under nitrogen blanketing. Conditions consisted in a barrel temperature of 200 °C and a crew-speed of 150 rpm (co-rotating mode) with a residence time of 5 min thanks to recirculation. Once cold, recovered strands were pelletized to obtain pellets of 3 mm.

Sheets of 200 μm were obtained by compression moulding dried (as

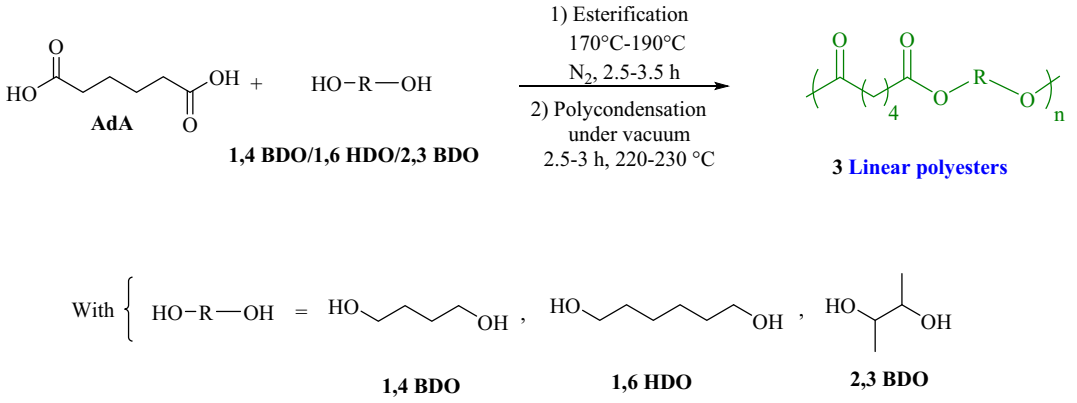

Scheme 1. Synthesis route of linear aliphatic polyesters

described above) pellets. A press (LP-S-50, Labtech) was used at 200 °C. Conditions were as follows: preheating time of 2 min, 3 degassing of 1 s, 3 min of compression at 50 bar followed by a cooling at 18 °C and 50 bar for 5 min.

2.4. Polymer characterization

All characterization methods are summarized in the Supplementary Information data.

3. Results and discussion

3.1. Characterization of the linear homopolyesters

3.1.1. Structural characterization of linear polyesters

The present work involves the synthesis of three fully biobased linear polyesters via two-stage melt polycondensation procedure (esterification and polycondensation) as depicted in Scheme 1. The followed route consisted to react the aliphatic diacid namely AdA with 1,4 BDO, 1,6 HDO or 2,3 BDO diol with the molar ratio of diacid/diol = 1:1.2. The esterification (first step of polymer synthesis) was performed under a controlled N_2 flow at temperature range of 170–190 °C and over a period of time oscillating between 2.5 and 3.5 h, depending on the prepared polyester type. The last stage, the polycondensation, was carried out under high-vacuum condition at 220–230 °C temperature range over a period of 2.5–3 h, relying on the polymer composition. It is worthy to note that the high vacuum application at a very slow rate was firmly recommended in the beginning of the second step of polycondensation. This procedure was aimed to prevent excessive foaming and also to minimize oligomers sublimation, which presents a potential problem that should be tackled during the melt polycondensation.

GPC measurements (Table S1) for AdA-1,4 BDO and AdA-1,6 HDO in THF revealed satisfactory number average molecular weights (M_w) of 12,700 and 9900 g/mol, respectively. It is worthy to note that once 2,3-BDO diol is used, the resulting sample namely, AdA-2,3 BDO, showed a significant drop in M_w, which was determined to be 4500 g/mol. This substantial difference in the molecular weight values could arise from the lower reactivity of secondary hydroxyl groups of 2,3 BDO compared to primary –OH functional groups of 1,4 BDO or 1,6 HDO. This is in good agreement with the results reported in Gao's study [36]. Therefore, an obvious correlation between 2,3 BDO chemical structure and its drastic effect on the low molecular weight decrease of the resulting materials was found. No trend could be established between the dispersity values of the prepared linear polyesters, varying in the 1.79–1.98 range (Table S1), and the structural features of the diols used herein.

^{1}H and ^{13}C NMR spectroscopies were used to ascertain the chemical structure of the three synthesized AdA based polyesters samples. All NMR spectra, depicted in Figs. S1-S3, were perfectly in agreement with the expected structures, where all signals are correctly assigned to the different protons and carbons of 1,4 BDO, 2,3 BDO and 1,6 HDO-based polyester's chain with AdA diacid as shown in Scheme S1. The spectra did not reveal any additional peak indicative of the presence of any impurity. The proton and carbon assignments and chemical shifts are summarized in Table S2.

To further assess the chemical structures of all prepared linear polyesters, FTIR data (Fig. S4) of the obtained materials were acquired as supportive evidence for the ^{1}H and ^{13}C NMR findings. All polymers spectra showed the characteristic absorption bands, originating from C═O and C-O-C stretching modes (ν C═O and ν C-O-C) of the ester group, at 1730 and 1245 cm^{-1}, respectively. Two weak peaks near to 2940 cm^{-1} and 2850 cm^{-1} were assigned to the C—H symmetrical and asymmetrical stretching modes of methylene groups of the aliphatic AdA diacid and (1,4 BDO, 1,6 HDO, or 2,3 BDO) diol moieties. To sum up, both FTIR and ^{1}H/^{13}C NMR data firmly corroborated that the aliphatic linear polyesters derived from fully renewable resources were successfully prepared.

3.1.2. Thermal properties of the linear polyesters

The thermal behavior of the AdA-based linear polyesters series was investigated by DSC and TGA. Special attention was put on the impact of their chemical structure on their thermal properties.

The DSC scans of the obtained materials derived from AdA dicarboxylic acids combined with the three different chain length aliphatic diols are presented in Fig. 1 (a and b), and the related thermal transition data, including the melting temperature (T_m) measured from the second heating scan, glass transition temperature (T_g), and crystallization temperature (T_c), were gathered in Table 1. According to these results, the AdA-based polyesters obtained from 1,4 BDO and 1,6-HDO were semicrystalline materials. It was found that with decreasing diol chain length from C_6 to C_4, the melting point of prepared samples slightly increases, wherein AdA-1,4 BDO and AdA-1,6 HDO exhibited T_m values of 58.3 and 56.4 °C, respectively. Moreover, the opposite trend in crystallization temperatures was discernible, that is, upon decreasing the chain-length of the incorporated diol units from C_6 (HDO) to C_4 (BDO), T_c decreased from 38.8 to 30.2 °C for AdA-1,6 HDO and AdA-1,4 BDO, respectively.

As can be seen in Fig. 1b, the glass transition temperatures of the prepared polyesters derived from 1,4 BDO and 1,6 HDO could not be readily detected. This is a consequence of the high crystallinity of these polymers. A further endothermic peak at 51.4 °C was revealed for AdA-1,4 BDO during the second heating scan. This dual melting endotherm could be ascribed to the melting-recrystallization process or to polymorphism in the polyester sample. This phenomenon is commonly detected in many polyesters.

The polyester derived from 2,3 BDO diol, AdA-2,3 BDO, exhibited a distinct thermal behavior. Indeed, they were completely amorphous, neither crystallization peak nor melting endotherm could be detected. The amorphous behavior of the polyester synthesized from 2,3 BDO lied to the quite significant repressing effect that the structure of the latter exerted, through its side methyl groups, on the destruction of chain's regularity, preventing thus the crystallization of the obtained materials. The inhibitory effect of 2,3 BDO on crystallization was confirmed in several previous studies in the literature [5]. This is in full accordance with what was reported in the present investigation.

As T_g value of all oligomers could not be obtained by DSC, the group contribution theory was applied to calculate approximate T_g values [37,38]. This concept is based on the sum of the contributions of the groups, atoms, or bonds that comprise the molecular structure of a monomer. This method has been extensively used for polymers with a linear structure [37,38].

3.1.3. Thermal degradation of linear polyesters

As the thermal degradation behavior and stability of polymers had a critical importance to determine their potential application, the thermogravimetric analysis (TGA) was carried out in a nitrogen atmosphere to assess the thermal stability of the synthesized linear polyesters and to compare the effect of the chain length of the introduced diol into the resulting polyesters' backbone.

The TGA thermograms recorded for the AdA-based polyesters in the 30–600 °C range are depicted in Fig. 2. Table 1 summarizes the decomposition parameters, calculated from TGA curves, such as the degradation temperature at 5 % and 10 % as well as the maximum decomposition temperature ($T_{d,\ max}$). All obtained linear polyesters underwent a single stage degradation and their remained residual weight at 500 °C ranges between 1.7 and 2.58 %. As can be seen, AdA-based polyesters showed to be thermally stable up to $T_{d,\ 5\%} > 264.6$ °C. It is obvious from Fig. 2 that the thermal stability is affected by the incorporated diol type. The effect of the diol unit on the considerable thermal stability increase showed the following order for AdA-based polymers: 1,4 BDO > 1,6 HDO > 2,3 BDO. The lowest value of onset decomposition temperature for AdA-2,3 BDO compared to the other two polyesters (264.6 °C vs 292 °C and 311.8 °C for AdA-1,6 HDO and AdA-1,4 BDO, respectively) could be mainly associated with the less reactive

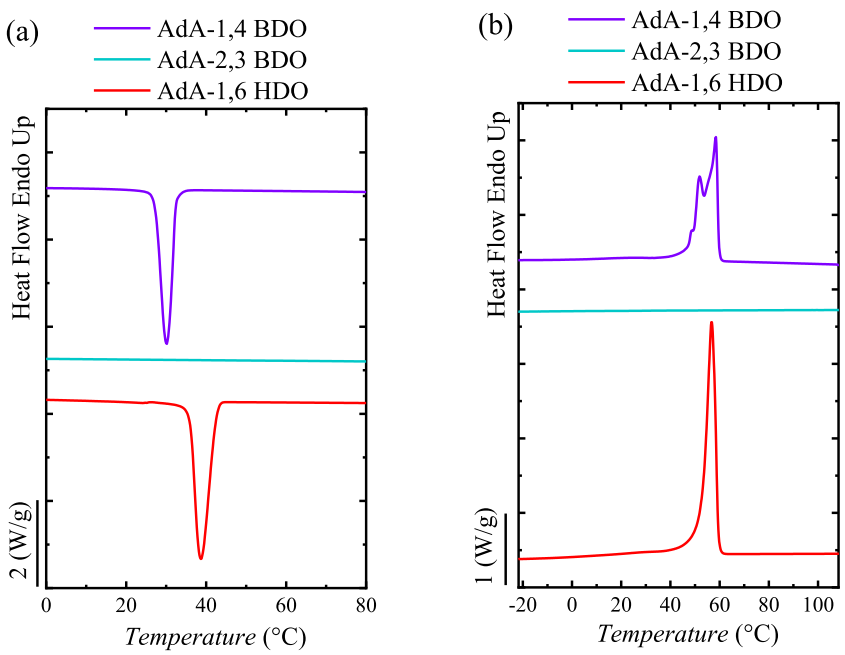

Fig. 1. DSC scans of the prepared linear polyesters derived from adipic acid in combination with 1,4 BDO, 2,3 BDO, and 1,6 HDO diols: (a) first cooling scan, and (b) second heating scan.

Table 1
Thermal properties of the prepared linear polyesters derived from AdA diacid in combination with 1,4 BDO, 1,6 HDO, and 2,3 BDO diols.

Samples	$T_{d,\ 5\%}$	$T_{d,\ 10\%}$	$R_{\ 500\ °C}$ (%)	T_g[a] (°C)	T_m (°C)	T_c (°C)
AdA-1,4 BDO	311.8	332.1	1.89	−10.1	58.3	30.2
AdA-2,3 BDO	264.6	322.6	2.58	15.9	–	–
AdA-1,6 HDO	292	316.1	1.70	−18.7	56.4	38.8

[a] Calculated by the group contribution theory.

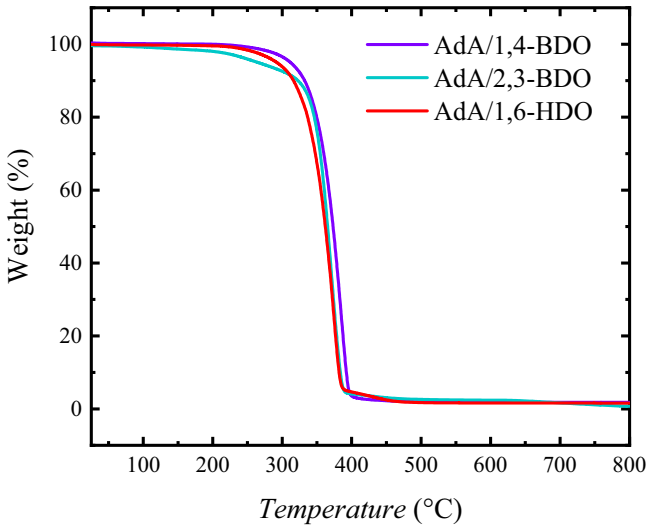

Fig. 2. TGA thermograms of prepared linear AdA-based polyesters in combination with 1,4 BDO, 1,6 HDO, and 2,3 BDO diols.

secondary hydroxyl groups of 2,3 BDO compared with those of the primary diols, 1,4 BDO and 1,6 HDO. This means that using 2,3 BDO building block the polymerization became more difficult to take place, and polymers having poor thermal stability were produced. This finding is in good agreement with what was reported in a previous study by Gao et al. [36]. It is worth mentioning that polyester sample, prepared from AdA and bearing short-chain diol (1,4 BDO) exhibit superior thermal stability than polymers bearing longer-chain diol (1,6-HDO): 311.8 °C vs 292 °C. This outcome is in full accordance with what reported in Hu's work [39].

3.2. PLLA based blends characterization

3.2.1. Tensile tests

The stress–strain curves are shown in Fig. 3 and data are collected in Table S3. Results showed that neat PLLA was quite brittle compared to plasticized blends. Neat PLLA showed 6 % elongation at break which was consistent with the values of 5–9 % that have been reported in the literature [40]. By plasticizing PLLA, the elongation value remarkably went up to 25–50 % depending on the oligomer esters type. In addition, while plasticizer allowed to increase elongation at break, tensile strength decreased differently depending on plasticizer type.

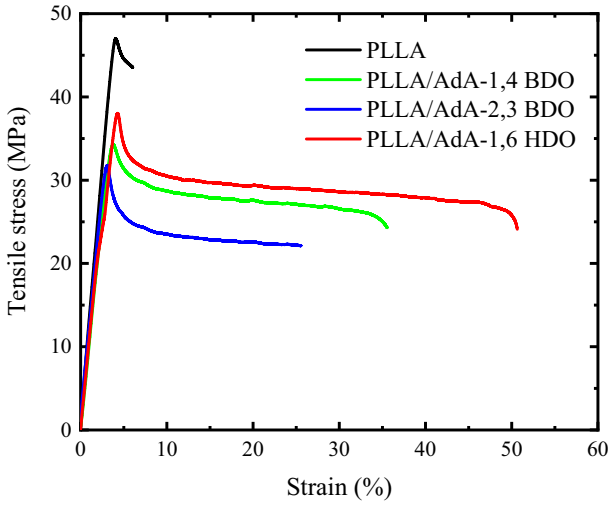

Fig. 3. Representative stress–strain curves for PLLA and plasticized PLLAs.

Interestingly, the tensile strength trend followed that of plasticizers molecular weight.

$$PLA > AdA-1,6\ HDO > AdA-1,4\ BDO > AdA-2,3\ BDO$$

However, surprisingly, elongation at break of short chain plasticizers-based blends were lower than that of longer ones. This result could not be related to crystallinities of moulded part which were amorphous. The elongation at break was in good agreement with T_g of the plasticizers; the lower the T_g of the plasticizer led to higher ultimate elongation in the plasticized PLLAs.

Santos et al. had studied PLA plasticized by oligoesters and found unremarkable increases in the elongation at break (from 3 % for neat PLA and 5.6 % for PLA/oligoester) [41].

3.2.2. DMA measurements on PLLA based blends

After PLLA has been blended with 10 wt% of various types of AdA-based linear polyesters plasticizers, samples were moulded in thin films on which DMA experiments were run. Results are presented in Fig. 4a and b. It could be observed that the introduction of 10 wt% of plasticizers did not drastically change the viscoelastic behavior of blend versus that of neat PLLA. Indeed, below 50 °C, no differences in storage modulus E' can be observed, indicating that at those levels of incorporation, the plasticizers do not significantly lower PLLA rigidity. Differences were however observed for temperatures ranging between 50 °C and 90 °C. In this domain, the onset temperatures at which storage modulus started decreasing were lower for plasticized PLLAs.

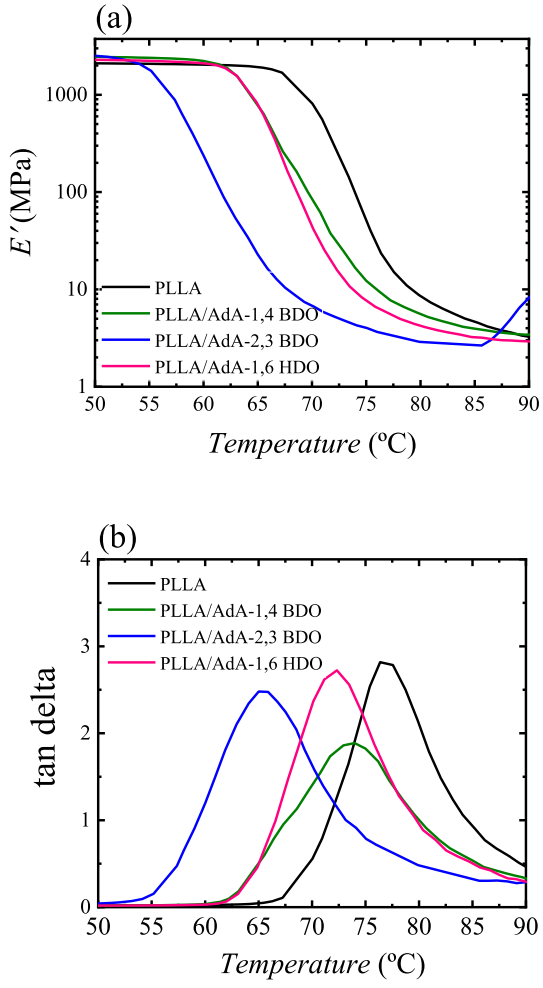

Fig. 4. (a) Evolution of storage modulus E' with temperature and (b) evolution of loss factor tan δ with temperature of plasticized PLLA blends.

This observation was also expressed in the variations of tan δ. Fig. 4b shows T(alpha), the main viscoelastic transition measured when following tan(delta). Only one T(alpha) is observed for all plasticized PLLAs, suggesting PLLA/plasticizers miscibility. As expected, plasticized PLLA blends presented lower T(alpha) temperatures when compared to neat PLLA. Indeed, T(alpha) was found to be 77 °C for neat PLLA, 74 °C for PLLA/AdA-2,3 BDO, 72 °C for PLLA/AdA-1.6 HDO and 65 °C for PLLA/AdA-1.4 BDO. Interestingly, results followed the same trend than that of plasticizers molecular weight:

$$AdA-1,4\ BDO > AdA-1,6\ HDO \gg AdA-2,3\ BDO$$

3.2.3. Non-isothermal DSC experiments on plasticized PLLAs

The non-isothermal crystallization and melting behavior of neat PLLA and its blends are presented in Fig. 5a and b. The related thermal transition data, measured from the second heating scan, including the melting temperature (T_m), glass transition temperature (T_g), and cold crystallization temperature (T_{cc}), are gathered in Table 2.

Fig. 5a shows that PLLA and plasticized PLLAs were not able to crystallize from the melt during cooling at 10 °C/min due to the slow overall non-isothermal crystallization rate of PLLA [3]. The second heating scans, Fig. 5b, show glass transitions, cold-crystallization exotherms, and melting endotherms for neat PLLA and all blends, respectively. All samples were able to crystallize when heated from the glassy state because of the enhanced nucleation process that occurs in PLLA during vitrification.

The neat PLLA sample showed a single melting endotherm, however all blends samples showed bimodal melting endotherms (with two melting points). This bimodal melting behavior could be a consequence of recrystallization during the heating run [14,42] and/or the presence of two crystalline forms [43,44]. The WAXS results discussed below proved the existence of two crystalline forms, α and α' in PLLA/AdA-1.6 HBO and PLLA/AdA-2,3 BDO samples.

Table 2 shows that all blends samples had lower cold crystallization temperatures (T_{cc}) than neat PLLA indicating a higher nucleating capacity of blends as compared to neat PLLA. This higher nucleation capacity was possibly due to the plasticizing effect of AdA-based linear polyester on the neat PLLA. These changes in the nucleation density will be discussed in detail below.

The melting temperatures of the blends (second melting peak) were slightly higher (around 1–3 °C) than the melting temperature of neat PLLA (with its single melting peak). The reason for such slight increase in melting points was not clear, although it could be connected with the enhanced cold crystallization capacity of the material in the blends.

Data gathered in Table 2 showed that for the neat PLLA and plasticized PLLAs, the cold crystallization (ΔH_{cc}) and melting enthalpies ($\Delta H_{m1} + \Delta H_{m2}$) values were nearly identical within the 10 % measurement error, indicating that all crystallization processes were accomplished during heating and samples did not crystallize at all during the cooling runs.

The single glass transition temperatures (T_g) of neat PLLA and its blends with AdA-based polyesters were well visible during the heating scans (Fig. 5b). In general, the DSC curves of neat PLLA and all blends with AdA-based polyesters exhibit one T_g value, which indicates that the blend system would be miscible [45]. The neat PLLA showed a T_g around 63 °C, however in the blended PLLA with AdA-based polyester, T_g values decreased to 52–56 °C in view of the plasticizing efficiency of the linear polyesters. Similar depression in glass transition values in comparison to neat PLLA chains have been reported for related polymer blends [46–48].

As the blended polyesters are miscible with PLLA and the amount added is only 10 %, the AdA-based polyester plasticizers are not able to crystallize in the blend. The crystallization and melting processes observed in Fig. 5b showed that the plasticizer didn't crystallize and only PLLA cold crystallization could be observed. These observations could be explained by the combination of small plasticizer quantities and

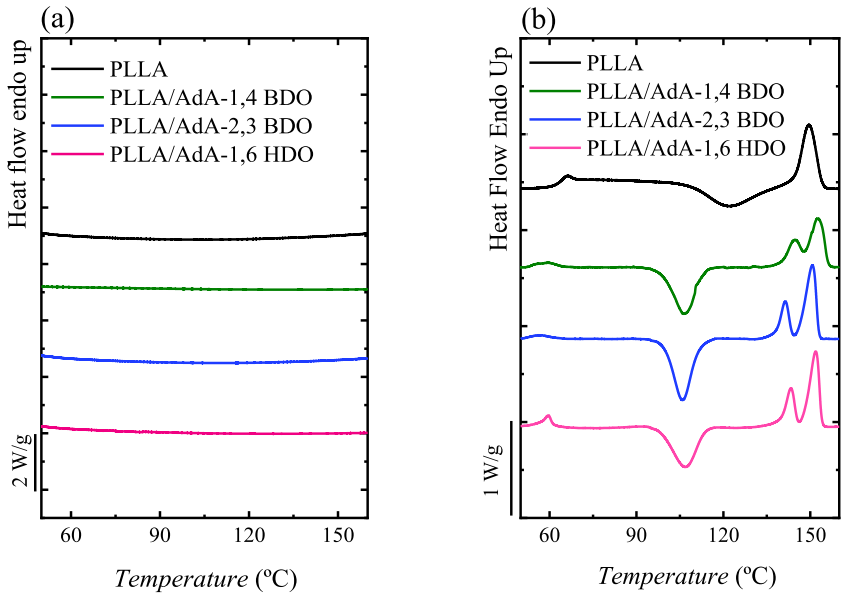

Fig. 5. (a) Cooling DSC scans from the melt at 10 °C/min, and (b) subsequent heating scans at 10 °C/min for the indicated samples.

Table 2
Thermal properties of PLLA and blends samples. All values were obtained from the DSC second heating runs shown in Fig. 5.

	T_{m1} (°C)	ΔH_{m1} (J/g)	T_{m2} (°C)	ΔH_{m2} (J/g)	T_{cc} (°C)	ΔH_{cc} (J/g)	T_g (°C)
PLLA	149.6	23.7	–	–	121.6	24.0	63.2
PLLA/AdA-1,4 BDO	152.6	18.5	144.7	7.7	106.4	30.9	53.6
PLLA/AdA-2,3 BDO	150.7	18.6	141.4	7.2	105.9	32.1	52.0
PLLA/AdA-1,6 HDO	151.9	18.9	143.0	8.9	106.8	31.5	56.3

blend components miscibility.

To study the crystalline structure of the neat PLLA and PLLA/AdA-based blends samples, WAXS experiments were performed at room temperature for melt-crystallized samples. Fig. 6 shows WAXS scans of the neat PLLA and the PLLA/AdA-1,6 HDO, PLLA/AdA-1,4 BDO, and PLLA/AdA-2,3 BDO blends, after crystallization at $T_c = 125$ °C for 2 h.

According to Fig. 6a, all samples showed one strong diffraction peak at $2\theta = 16.6°$ and two weak diffraction peaks at $2\theta = 14.8°$ and $19.0°$ corresponding to the 010, 100/200, and 203 reflections of the stable α form of PLLA, respectively [49–51]. As it was expected for the neat PLLA sample, only the α phase of PLLA was able to form at crystallization temperatures above 120 °C with an orthorhombic unit cell [49,52,53]. Fig. 6b shows an enlargement of WAXS patterns shown in Fig. 6a. In the case of PLLA/AdA-1,4 BDO blend, the plasticizer did not change the PLLA main crystal structure. In the case of PLLA blended with PLLA/AdA-2,3 BDO and AdA-1,6 HDO, a peak appears at $2\theta = 24.2°$ that corresponds to α' form crystal (less ordered than α form crystal), hence in these samples a mixture of α and α' phases exists. Moreover, PLLA/AdA-1,6 HDO shows a new peak at $2\theta = 21.50°$ whose origin is unknown, as it is not related to the presence of α' crystals. This merits further crystallographic studies which are outside the scope of the present paper.

3.2.4. Nucleation and growth rates from the melt state

To study the plasticization effect of PLLA by linear AdA based polyesters on the nucleation and growth of PLLA spherulites, the growth rate and nucleation density were determined by PLOM. Micrographs were collected during isothermal crystallization from the melt state at different temperatures for spherulitic size and nuclei quantity measurements. We performed PLOM observation by crystallization from the molten state because when PLOM micrographs were taken from the glassy state crystallization, a granular texture was observed (an example result for the neat PLLA is shown in Fig. S6). This microspherulitic morphology was expected from the enhanced nucleation that occurs when the crystallization proceeds from the glassy state preventing nuclei counting and spherulitic growth measurements.

Fig. 7 shows the spherulite morphology of neat PLLA and its blends with AdA-based linear polymers after isothermal crystallization at 120 °C for 20 min. Typical PLLA negative spherulites were observed. As it can be seen in Fig. 7, among the samples under this study, the smallest spherulites belonged to neat PLLA, and the largest ones were formed when PLLA was blended with AdA-2,3 BDO.

Fig. 8 shows the data collected from the captured micrographs during isothermal crystallization at the indicated temperatures for PLLA/AdA-1,4 BDO sample as a representative set of nucleation kinetics data. The nucleation kinetics data for the rest of samples was presented in Figs. S8 and S9. In general, when the crystallization is performed from the molten state, for neat PLLA and its blends with AdA-based polymer, as the crystallization temperature decreased the nucleation density ρ_{nuclei} increased, and the influence of crystallization temperature on the ρ_{nuclei} in the blends was stronger than in neat PLLA (Fig. 8a). The PLLA/AdA-2,3 BDO blend showed the lowest nucleation density among all samples resulting in the largest spherulites (also see Fig. 7c).

In all cases, and for all different crystallization temperatures, there was a nearly linear increase of the radius with time as seen in Fig. 5b and Fig. S8. Xiao et al. reported PLA plasticized with triphenyl phosphate (TPP) and found that spherulite growth rates for PLA/TPP were higher than those of neat PLA [51].

The nucleation rate (I) presented in Fig. 9a versus T_c was determined from the initial slope of the nucleation density versus time plots (such as that in Fig. 9a), where a straight line could be fitted to the experimental data (Fig. 9a and S8 plots). Neat PLLA showed the highest nucleation rate from the melt in comparison to the blends. By adding 10 % of any AdA-based polymer, a remarkable drop in the nucleation rate from the

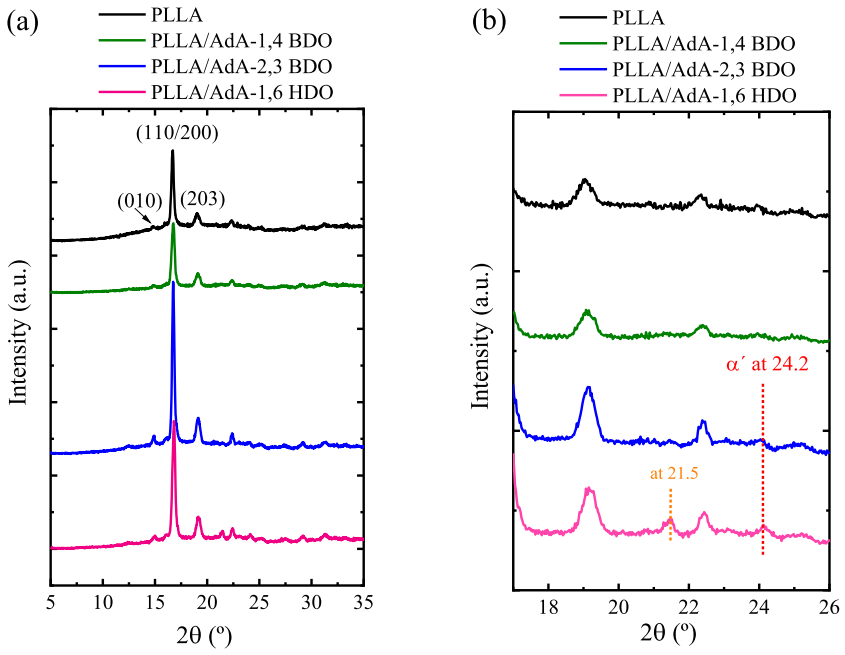

Fig. 6. (a) WAXS patterns in the full angular range examined and (b) enlarged WAXS patterns of the neat and blend PLLA samples after isothermal crystallization from the melt at 125 °C.

melt occurred at a same crystallization temperature (see Fig. S9). At these relatively high crystallization temperatures, the primary nucleation effect was weakened by the plasticization effect of the linear polymer additive, which could be a result of an excess chain mobility that enhances chain detachment rates in comparison to chain attachment rates to existing heterogeneities. The nucleation of the PLLA melt occurs by heterogeneous nucleation.

The experimental growth rate G (μm/min) values were calculated from the slope of spherulite radius versus *time* (e.g., Fig. 8b) and plotted versus the isothermal crystallization temperatures in Fig. 9b. The spherulitic growth rate, G, shows a bell-shaped temperature dependence, as a result of the competition between secondary nucleation control at higher temperatures and diffusion control at lower temperatures. The growth rate displays a maximum at around 125 °C for neat PLLA and its blends [54].

The incorporation of AdA-based linear polymer units had an incremental impact on the growth rate, G, of neat PLLA spherulites. The spherulite growth rate G increased with polyester addition, probably because of less restricted polymer chain mobility (inducing faster and easier polymer diffusion) in the blends sample as these blends showed a lower T_g value in comparison to neat PLLA (see Table 2 for T_g values). For this reason, the increase in G was particularly significant in the left-hand side of the bell-shaped curve, which was the one dominated by diffusion.

The Lauritzen and Hoffman (LH) theory [54] was employed to determine the energetic parameters related to the growth process, according to the following exponential equation:

$$G = G_0 exp\left[\frac{-U^*}{R(T_c - T_0)}\right]\left[\frac{-K_g^G}{fT\left(T_m^0 - T_c\right)}\right] \quad (1)$$

where G_0 is the growth rate constant and almost independent of temperature, U^* is the transport activation energy which characterizes molecular diffusion across the interfacial boundary between melt and crystals (taken as a constant value of 1500 cal/mol). T_c is the crystallization temperature and T_0 is a hypothetical temperature at which all chain movements freeze ($T_0 = T_g - 30$ °C); T_m^0 is the thermodynamic equilibrium melting temperature of the polymer and R is a gas constant.

Plotting $lnG + \frac{-U}{R(Tc-T0)}$ versus $1/T_c(\Delta T)f$ gave a straight line and its slope and intercept were equal to K_g^G and G_0 respectively. The work done by the polymer chains to form a fold was given by $q = 2a_0b_0\sigma_e$. Examples of L-H plots for neat PLLA can be found in Fig. S10. The dashed lines in Fig. 9b correspond to fittings to Eq. (1). Table 3 shows that K_g^G, a parameter proportional to the energy barrier for the crystal growth of PLLA, decreased with AdA-based plasticizer addition in comparison with the value for neat PLLA. Similar trends were observed for the fold surface free energy σ_e and for the work done to form folds, q. The values of these three energetic parameters (K_g^G, σ_e and q) varied as expected considering the trends observed in spherulitic growth rate in Fig. 9b. As the rate of spherulitic growth increased, these energetic parameters decreased as the plasticizing action of the added AdA-based polyesters increased.

3.2.5. *Overall isothermal crystallization from the glassy state*

Isothermal DSC experiments can be used to determine the overall crystallization kinetics that includes both nucleation and growth. Fig. S11 shows the experimental isothermal crystallization from the glassy state of the neat PLLA and its blend with AdA-based polymers. As it can be seen in Fig. S11, by applying the isothermal protocol explained in the experimental part (also the protocol can be seen in Fig. S5) to perform isothermal crystallization experiments from the glassy state, we were able to determine the overall isothermal crystallization kinetics for neat PLLA and its blends with linear AdA-based polyesters.

The overall crystallization rate (reported as the inverse of the crystallization half time ($1/\tau_{50\%}$)) as a function of T_c for all samples is shown in Fig. 10a. For neat PLLA and its plasticized blends, the overall crystallization rate increased with crystallization temperature and a maximum value was reached at around 115 °C. After reaching the maximum value at 115 °C, $1/\tau_{50\%}$ decreases with T_c. This bell shape curve is typical of polymer crystallization, while the low T_c range is dominated by diffusion, while the high T_c range is governed by nucleation (both primary and secondary nucleation in this case). The PLLA/AdA-based polymers blends showed a much faster crystallization rate than neat PLLA. For instance, comparing the blends at a constant T_c value of 115 °C, the PLLA blends show four times faster crystallization rate as compared to neat PLLA. These results were mainly connected to

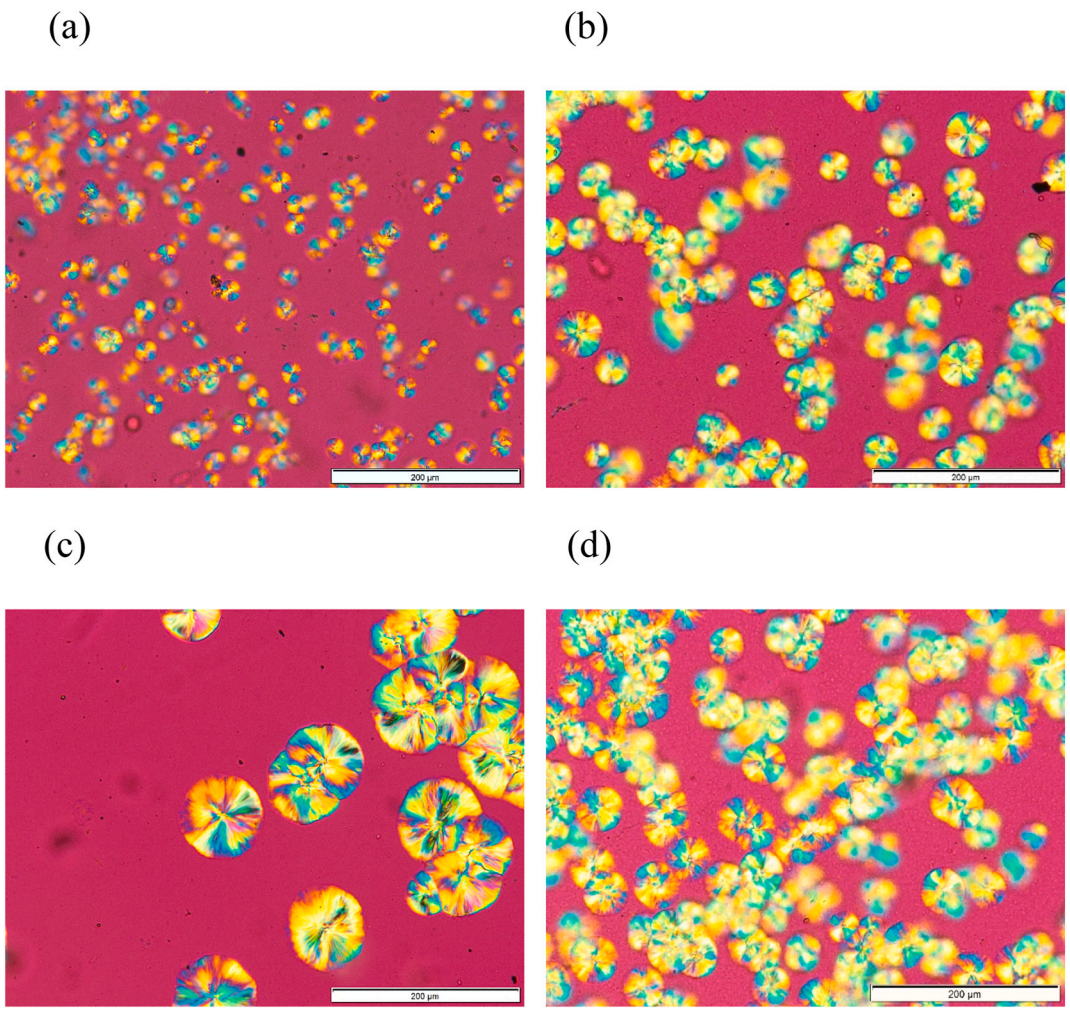

Fig. 7. Spherulitic morphology of the melt crystallized polymers samples observed by PLOM, at a crystallization temperature of 120 °C after 20 min for (a) neat PLLA, (b) PLLA/AdA-1,4 BDO (c) PLLA/AdA-2,3 BDO (d) PLLA/AdA-1,6 HDO. Scale bar: 200 µm.

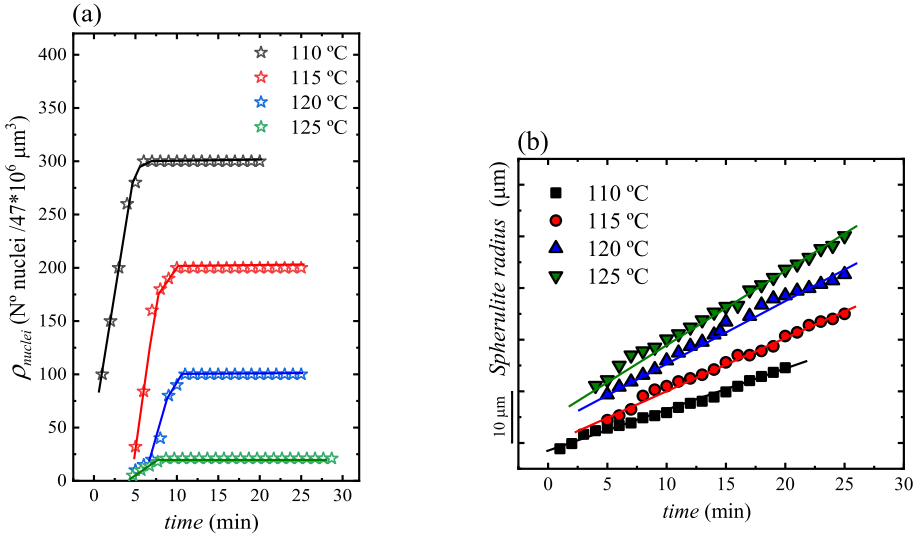

Fig. 8. (a) Nucleation density and (b) spherulite radius as a function of time for a PLLA AdA-1,4 BDO sample at different T_c values.

the plasticizing effect of the linear AdA polyester on PLLA.

Fig. 10b shows the inverse of the induction time for the primary nucleation ($1/t_0$) from the glassy state as a function of T_c. t_0 is the incubation time, or the time needed for nucleation before any crystallization or growth can proceed. Therefore, $1/t_0$ is proportional to the primary nucleation rate from the glassy state. As it can be seen in

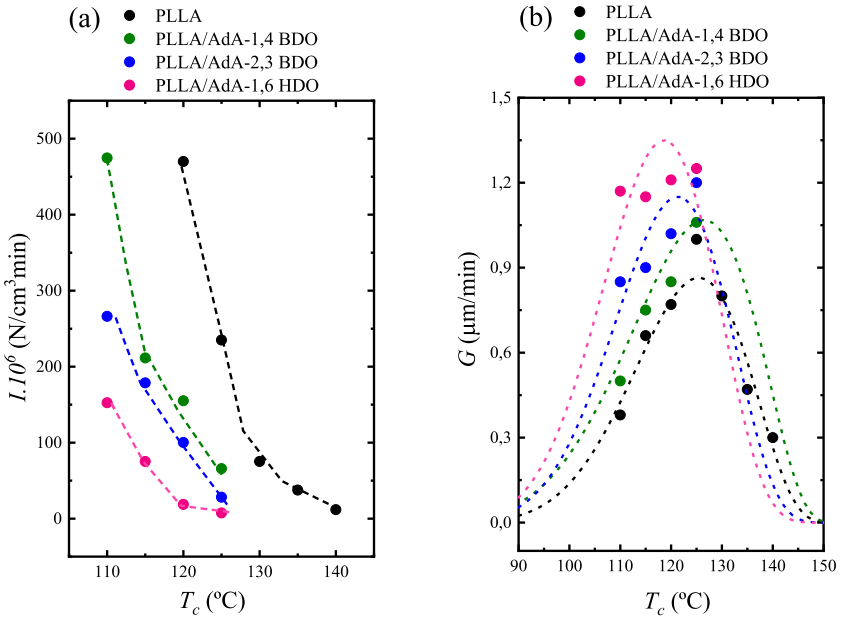

Fig. 9. (a) Nucleation rate as a function of the crystallization temperature and (b) spherulitic growth determined by PLOM for the indicated samples. The dashed lines are the fits to the Lauritzen–Hoffman (LH) theory, Eq. (1).

Table 3
Parameters obtained from fitting the PLOM data to the Lauritzen–Hoffman model.

Sample name	G_0 (cm/s)	K_g^G(K^2)	σ_e (erg/cm^2)	q (erg)
PLLA	0.146	8.62E+04	58	2.29E-13
PLLA/AdA 1,4 BDO	0.280	2.89E+04	19	0.87E-13
PLLA/AdA 2,3 BDO	0.678	6.00E+04	39	1.80E-13
PLLA/AdA 1,6 HDO	2.010	7.34E+04	48	2.20E-13

Fig. 10b, while neat PLLA had a lower $1/t_0$ value compared to its plasticized blends, PLLA/AdA-1,6 HDO showed the highest $1/t_0$ values. The addition of 10 % AdA-1,6 HDO to PLLA increased the nucleation from the glassy state, as chain mobility at temperatures close to vitrification (where long-range chain mobility is highly restricted) is also enhanced. It is interesting to stress that in the nucleation from the melt state (Fig. 9a), the opposite results were found because an excess in mobility (caused by plasticization) can decrease the primary nucleation in the melt.

The Lauritzen and Hoffman theory can also be applied to fit the overall crystallization data obtained by DSC measurements using following equation:

$$1/\tau_{50\%} = 1/\tau_{50\%} exp\left[\frac{U}{R(T_c - T_0)}\right]\left[\frac{-K_g^\tau}{fT(T_m^0 - T_c)}\right] \quad (2)$$

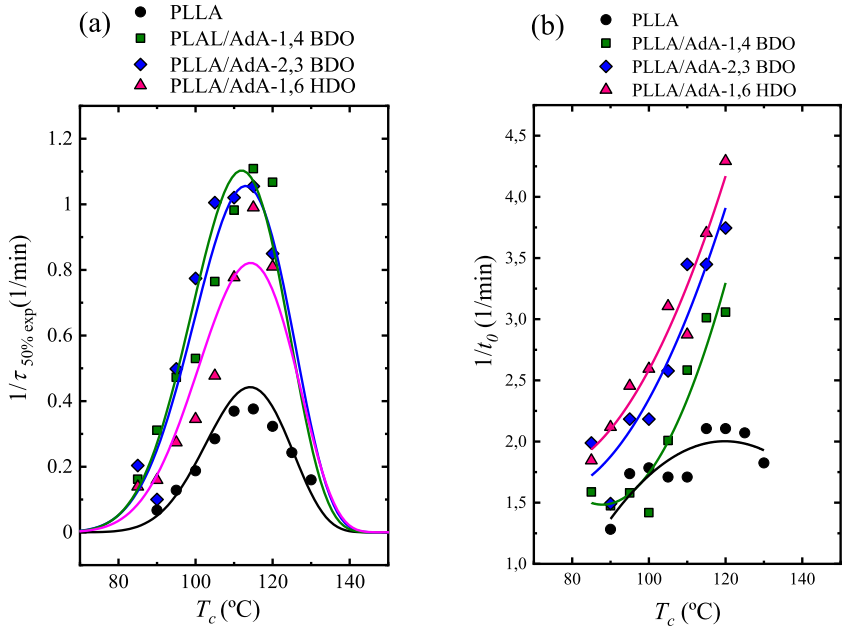

Fig. 10. (a) Overall crystallization rate and (b) primary nucleation rate, obtained by DSC for samples isothermally crystallized from the glassy state, as a function of *Tc*. The solid lines represent fits to the Lauritzen and Hoffman theory.

where most of the terms have been defined above. Here K_g^τ is a constant proportional to the energy barrier for both primary nucleation and spherulitic growth (secondary nucleation) and it is different from K_g^G (Eq. (1)) derived from growth rate and therefore proportional only to the energy barrier for growth. The solid lines in Figs. 10a represent fits to the Lauritzen-Hoffman theory. All the relevant parameters obtained from L-H equation are listed in Table 4.

A faster crystallization process from the glassy state is characterized by a lower energy barrier for nucleation and growth (i.e., lower K_g^τ, lower surface fold energy (σ_e), and a smaller work done by the chains to fold (q)). As anticipated, Table 4 showed that all these energetic parameters were lower for plasticized PLLA, even though the trends obtained for the blends did not show meaningful changes that could be correlated with the specific overall crystallization rate results observed in Fig. 10. When comparing the values in Tables 3 and 4, it is clear that the values obtained from fitting the L-H theory by PLOM are smaller than those obtain ed. by DSC. Indeed, the values reported in Table 3 take into account only the growth of spherulites, while Table 4 considers both nucleation and growth.

Xiao et al. [51] reported that the overall crystallization time for PLA/TPP blends decreased when compared with neat PLA, in view of the plasticizing action of TPP that increased mobility and reduced the T_g value.

3.2.6. Fitting of DSC isothermal crystallization data to the Avrami theory

The Avrami equation (Eq. (3)) can describe the primary overall crystallization process in polymers by the following equation [32]:

$$1 - Vc(t - t_0) = exp(-k(t - t_0)^n) \quad (3)$$

where V_c is the relative volumetric transformed fraction (as a function of time), t is the experimental time of crystallization, t_0 is the induction time for crystallization, k is the rate constant of isothermal crystallization, and n is the Avrami index for describing nucleation mechanism and crystal growth. We employed the Origin plug-in developed by Lorenzo et al. [32] to fit the Avrami equation to the experimental data. Fig. 11 shows a representative fit of Avrami theory for the crystallization of the PLLA/AdA-1,6 BDO sample at 100 °C. The Avrami plot of the experimental data obtained during crystallization of the neat PLLA at 110 °C is presented in Fig. S12, and the data from the Avrami fitting model for all samples are collected in Table S4.

Fig. 11a shows the Avrami plot (derived from Eq. (3)) that is linearized by the double logarithmic scale of the axis, within 3–20 % conversion range that corresponds to the early stage of primary crystallization, before any spherulitic impingement takes place. The Avrami index, n, obtained as well as the k value and the correlation coefficient for the fit, R^2, are included in the plot for one example. The normalized experimental heat flow data is well modeled by the Avrami fit using the obtained values from Eq. (3), and a comparison between experimental data and predictions from the Avrami equation is plotted in Fig. 11b.

Table 4
Values obtained by fitting the L-H theory to experimental DSC overall crystallization data. Parameter proportional to the energy barrier for secondary nucleation (K_g^τ), fold surface energy (σ_e), and work done by the chain to perform a fold (q).

Sample name	$1/\tau_0$ (1/s)	K_g^τ(K^2)	σ_e (erg/cm^2)	q (erg)	R^2
PLLA	3.84E+04	10.1E+04	66	3.04E-13	0.995
PLLA/AdA-1,4 BDO	2.39E+04	9.44E+04	62	2.83E-13	0.989
PLLA/AdA-2,3 BDO	0.57E+04	7.81E+04	51	2.34E-13	0.910
PLLA/AdA-1,6 HDO	1.12E+04	8.50E+04	64	2.84E-13	0.892

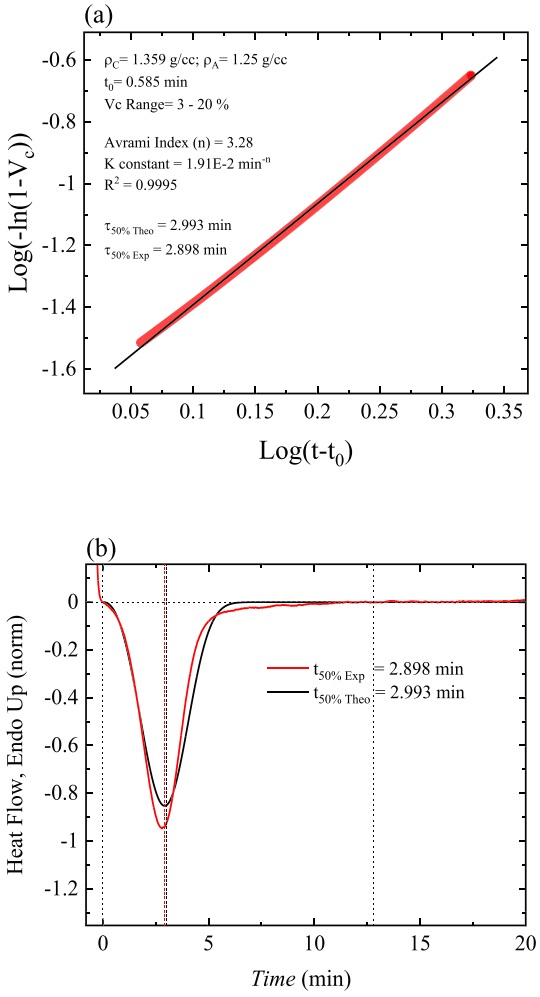

Fig. 11. An example of Avrami plots of the data obtained during crystallization of PLLA/AdA 1,6 BDO at 100 °C. (a) Avrami plot of the experimental data obtained during crystallization. (b) Normalized heat flow experimental data during crystallization compared to the data predicted by the Avrami model.

Fig. 12 shows the kinetic parameters of overall crystallization as a function of the crystallization temperature for neat PLLA and its blends with AdA-based linear polymers. In Fig. 12a, the inverse of the experimental half-crystallization ($1/\tau_{50\%.\,exp}$) data is plotted. The solid lines in Fig. 12a correspond to the L-H fitting. The $k^{1/n}$ values were calculated from the Avrami theory parameter by elevating k (isothermal crystallization rate constant) to $1/n$ (1/Avrami index), and they were proportional to the overall crystallization rate. The $k^{1/n}$ values are plotted versus T_c in Fig. 12b and also fitted to the L-H theory (solid lines). The significant similarity between Fig. 12a and Fig. 12b is a consequence of the well-fitted Avrami equation to the experimental overall crystallization rate data until approximately 50 % conversion.

Fig. 12c shows the values of the Avrami index n as a function of T_c. The values fluctuated between 1.5 and 3.5. As it was described earlier, the overall isothermal crystallization kinetics by DSC was determined from the glassy state, therefore the nucleation density was remarkably improved. At lower crystallization temperature the n value is nearly 3 indicating that spherulites grew instantaneously, as expected from the high nucleation rate from the glassy state. At a higher crystallization temperature, n values decreased to nearly 2, which may be explained by a morphological change from spherulites to axialites.

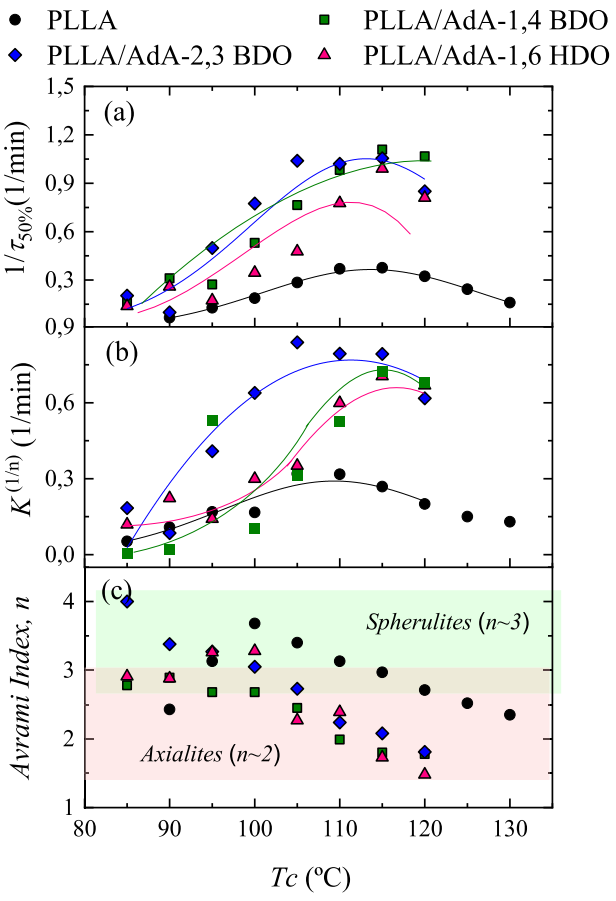

Fig. 12. (a) Overall crystallization rates, expressed as the inverse of the experimentally determined half-crystallization times, (b) normalized crystallization constant from the Avrami model and (c) Avrami index for the indicated neat PLLA and plasticized samples as a function of crystallization temperature. Solid lines in (a) and (b) correspond to the fit of the Lauritzen–Hoffman (L-H) theory.

4. Conclusions

This present study explored the effect of biobased aliphatic polyester plasticizers on PLLA. While the thermomechanical and mechanical properties were evaluated, a special focus was put on the nucleation and crystallization kinetics of neat and plasticized PLLA.

To this aim, three different biobased linear aliphatic AdA-based polyesters were successfully synthesized through the two-stage melt method (esterification and polycondensation). AdA-1,4 BDO and ADA-1,6 HDO showed a semicrystalline behavior, however ADA-2,3 BDO was totally amorphous.

Subsequently, 10 wt% of these polyesters were used as a plasticizer for PLLA in order to enhance its crystallization rate. Plasticized PLLA blends displayed a single T_g value, suggesting full blend miscibility, that shifted to lower temperatures. WAXS results demonstrated that the presence of AdA/ 1,4 BDO and AdA/ 2,3 BDO plasticizers were able to form both α and α′ crystal structures of PLLA.

Tensile tests showed PLLA blends plasticized with 10 wt% AdA-1,6 HDO presented the highest improvement in toughness with an 8-fold increase in elongation at break.

Isothermal crystallization from the melt state indicated that the addition of only 10 wt% of any plasticizer to PLLA caused a significant dramatic increase to the spherulitic growth rate. However, plasticization led to a decrease in the nucleation rate and nucleation density. In addition, it was found that the plasticizer based longer aliphatic chains monomers (AdA-1,6 HDO) caused a higher impact on the spherulite growth rate of PLLA. This could probably be connected to easier polymer diffusion. Plasticizer incorporation within PLLA caused a remarkable increase in the overall crystallization rate that derived from a lower free energy barrier for both nucleation and growth of PLLA crystals that initiated their crystallization from the glassy state. Moreover, the plasticizers based on shorter aliphatic chains monomers had a larger impact on PLLA overall crystallization rate.

CRediT authorship contribution statement

Maryam Safari: Data curation, analysis, writing original draft. Nejib Kasmi: Data curation, analysis, writing original draft. Carla Pisani: Data curation. Vincent Berthé: Investigation, Reviewing-Editing. Alejandro J. Müller: Conceptualization, Supervision, Reviewing-Editing Youssef Habibi: Conceptualization, Supervision, Reviewing-Editing.

Acknowledgements

The authors are grateful to the Luxembourg National Research Fond (FNR) for financial support (CATBIOSE project INTER/ANR 15/ 9903334). We would like to acknowledge Coraline Sirot, Régis Vaudemont and Benoît Marcolini who continuously provide a friendly and supportive environment to help us conduct our work. We acknowledge the financial support from the BIODEST project; this project has received funding from the European Union's Horizon 2020 research and innovation program under the Marie Skłodowska-Curie Grant Agreement No. 778092. This work has also received funding from the Basque Government through grant IT1309-19.

Appendix A. Supplementary data

Supplementary data to this article can be found online at https://doi.org/10.1016/j.ijbiomac.2022.06.056.

References

[1] S. Saeidlou, M.A. Huneault, H. Li, C.B. Park, Poly(lactic acid) crystallization, Prog. Polym. Sci. 37 (2012) 1657–1677, https://doi.org/10.1016/j.progpolymsci.2012.07.005.
[2] L. Fambri, C. Migliaresi, Crystallization and thermal properties, in: R. Auras, L. T. Lim, S.E.M. Selke, H. Tsuji (Eds.), Crystallization and Thermal Properties in Poly (Lactic Acid): Synthesis, Structures, Properties, Processing, and Applications, John Wiley & Sons Inc, New Jersey, 2010, pp. 113–124.
[3] A.J. Müller, M. Ávila, G. Saenz, J. Salazar, Crystallization of PLA-based materials, in: A. Jimenes, M. Peltzer, R. Ruseckaite (Eds.), Poly(lactic acid) Science and Technology: Processing, Properties, Additives and Applications, Royal Society of Chemistry, Oxfordshire, 2015, pp. 66–98.
[4] H. Tsuji, H. Takai, S.K. Saha, Isothermal and non-isothermal crystallization behavior of poly(l-lactic acid): effects of stereocomplex as nucleating agent, Polymer 47 (2006) 3826–3837, https://doi.org/10.1016/j.polymer.2006.03.074.
[5] G. Perego, G.D. Cella, C. Bastioli, Effect of molecular weight and crystallinity on poly(lactic acid) mechanical properties, J. Appl. Polym. Sci. 59 (1996) 37–43, https://doi.org/10.1002/(SICI)1097-4628(19960103)59:1<37::AID-APP6>3.0.CO;2-N.
[6] H. Li, M.A. Huneault, Effect of nucleation and plasticization on the crystallization of poly(lactic acid), Polymer 48 (2007) 6855–6866, https://doi.org/10.1016/j.polymer.2007.09.020.
[7] N. Ljungberg, B. Wesslén, The effects of plasticizers on the dynamic mechanical and thermal properties of poly(lactic acid), J. Appl. Polym. Sci. 86 (2002) 1227–1234, https://doi.org/10.1002/app.11077.
[8] S. Jacobsen, H.G. Fritz, Plasticizing polylactide—the effect of different plasticizers on the mechanical properties, Polym. Eng. Sci. 39 (1999) 1303–1310, https://doi.org/10.1002/pen.11517.
[9] O. Martin, L. Avérous, Poly(lactic acid): plasticization and properties of biodegradable multiphase systems, Polymer 42 (2001) 6209–6219, https://doi.org/10.1016/S0032-3861(01)00086-6.
[10] Y. Hu, Y.S. Hu, V. Topolkaraev, A. Hiltner, E. Baer, Aging of poly(lactide)/poly (ethylene glycol) blends. Part 2. Poly(lactide) with high stereoregularity, Polymer 44 (2003) 5711–5720, https://doi.org/10.1016/S0032-3861(03)00615-3.
[11] L. Jiang, M.P. Wolcott, J. Zhang, Study of biodegradable polylactide/poly(butylene adipate-co-terephthalate) blends, Biomacromolecules 7 (2006) 199–207, https://doi.org/10.1021/bm050581q.
[12] W.C. Lai, W.B. Liau, T.T. Lin, The effect of end groups of PEG on the crystallization behaviors of binary crystalline polymer blends PEG/PLLA, Polymer 45 (2004) 3073–3080, https://doi.org/10.1016/j.polymer.2004.03.003.

[13] M. Baiardo, G. Frisoni, M. Scandola, M. Rimelen, D. Lips, K. Ruffieux, E. Wintermantel, Thermal and mechanical properties of plasticized poly(L-lactic acid), J. Appl. Polym. Sci. 90 (2003) 1731–1738, https://doi.org/10.1002/app.12549.
[14] Z. Kulinski, E. Piorkowska, Crystallization, structure and properties of plasticized poly(l-lactide), Polymer 46 (2005) 10290–10300, https://doi.org/10.1016/j.polymer.2005.07.101.
[15] L.V. Labrecque, R.A. Kumar, V. Davé, R.A. Gross, S.P. McCarthy, Citrate esters as plasticizers for poly(lactic acid), J. Appl. Polym. Sci. 66 (1997) 1507–1513, https://doi.org/10.1002/(SICI)1097-4628(19971121)66:8<1507::AID-APP11>3.0.CO;2-0.
[16] N. Ljungberg, B. Wesslén, Preparation and properties of plasticized Poly(lactic acid) films, Biomacromolecules 6 (2005) 1789–1796, https://doi.org/10.1021/bm050098f.
[17] N. Ljungberg, T. Andersson, B. Wesslén, Film extrusion and film weldability of poly (lactic acid) plasticized with triacetine and tributyl citrate, J. Appl. Polym. Sci. 88 (2003) 3239–3247, https://doi.org/10.1002/app.12106.
[18] S. Jacobsen, H.G. Fritz, Filling of poly(lactic acid) with native starch, Polym. Eng. Sci. 36 (1996) 2799–2804, https://doi.org/10.1002/pen.10680.
[19] Z. Kulinski, E. Piorkowska, K. Gadzinowska, M. Stasiak, Plasticization of poly(L-lactide) with poly(propylene glycol), Biomacromolecules 7 (2006) 2128–2135, https://doi.org/10.1021/bm060089m.
[20] E. Piorkowska, Z. Kulinski, A. Galeski, R. Masirek, Plasticization of semicrystalline poly(l-lactide) with poly(propylene glycol), Polymer 47 (2006) 7178–7188, https://doi.org/10.1016/j.polymer.2006.03.115.
[21] J.M. Ferri, D. Garcia-Garcia, N. Montanes, O. Fenollar, R. Balart, The effect of maleinized linseed oil as biobased plasticizer in poly(lactic acid)-based formulations, Polym. Int. 66 (2017) 882–891, https://doi.org/10.1002/pi.5329.
[22] S.P. McCarthy R.A. Gross W. Ma Polyactic acid-based blends. Patent US5883199A (1999).
[23] Y. Yoshida S. Obuchi Y. Kitahara T. Watanabe H. Aihara T. Nakata K. Suzuki M. Ajioka Polylactic acid composition and film thereof. Patent EP0980894A1 1999.
[24] T. Kurose Impact-resistant polylactic acid resin composition. Patent JP2010126643A 2008.
[25] A. Díaz, R. Katsarava, J. Puiggalí, Synthesis, properties and applications of biodegradable polymers derived from diols and dicarboxylic acids: from polyesters to poly(ester amide)s, Int. J. Mol. Sci. 15 (2014) 7064–7123, https://doi.org/10.3390/ijms15057064.
[26] T. Debuissy, E. Pollet, L. Avérous, Synthesis of potentially biobased copolyesters based on adipic acid and butanediols: kinetic study between 1,4- and 2,3-butanediol and their influence on crystallization and thermal properties, Polymer 99 (2016) 204–213, https://doi.org/10.1016/j.polymer.2016.07.022.
[27] S. Gestí, A. Almontassir, M.T. Casas, J. Puiggalí, Crystalline structure of poly (hexamethylene adipate).Study on the morphology and the enzymatic degradation of single crystals, Biomacromolecules 7 (2006) 799–808, https://doi.org/10.1021/bm050860d.
[28] B. Xiao, M. Zheng, X. Li, J. Pang, R. Sun, H. Wang, X. Pang, A. Wang, X. Wang, T. Zhang, Synthesis of 1,6-hexanediol from HMF over double-layered catalysts of Pd/SiO2 + Ir–ReOx/SiO2 in a fixed-bed reactor, Green Chem. 18 (2016) 2175–2184, https://doi.org/10.1039/C5GC02228B.
[29] K.H. Kang, U.G. Hong, Y. Bang, J.H. Choi, J.K. Kim, J.K. Lee, S.J. Han, I.K. Song, Hydrogenation of succinic acid to 1,4-butanediol over Re–Ru bimetallic catalysts supported on mesoporous carbon, Appl. Catal. A-Gen. 490 (2015) 153–162, https://doi.org/10.1016/j.apcata.2014.11.029.
[30] X.J. Ji, H. Huang, P.K. Ouyang, Microbial 2,3-butanediol production: a state-of-the-art review, Biotechnol. Adv. 29 (2011) 351–364, https://doi.org/10.1016/j.biotechadv.2011.01.007.
[31] J. Han, A bio-based 'green' process for catalytic adipic acid production from lignocellulosic biomass using cellulose and hemicellulose derived γ-valerolactone, Energy Convers. Manag. 129 (2016) 75–80, https://doi.org/10.1016/j.enconman.2016.10.019.
[32] A.T. Lorenzo, M.L. Arnal, J. Albuerne, A.J. Müller, DSC isothermal polymer crystallization kinetics measurements and the use of the avrami equation to fit the data: guidelines to avoid common problems, Polym. Test. 26 (2007) 222–231, https://doi.org/10.1016/j.polymertesting.2006.10.005.
[36] Y. Gao, Y. Li, X. Hu, W. Wu, Z. Wang, R. Wang, L. Zhang, Preparation and properties of novel thermoplastic vulcanizate based on bio-based Polyester/Polylactic acid, and its application in 3D printing, Polymers 9 (2017) 694, https://doi.org/10.3390/polym9120694.
[37] D.W. Van Krevelen, in: Properties of Polymers: Correlations With Chemical Structure, Elsevier, Amsterdam, 1972, pp. 41–109.
[38] D.W. Van Krevelen, in: Properties of Polymers: Their Correlation With Chemical Structure: Their Numerical Estimation and Prediction From Additive Group Contributions, 4th ed., Elsevier, Amsterdam, 2009, pp. 71–130.
[39] K. Hu, D. Zhao, G. Wu, J. Ma, Synthesis and properties of polyesters derived from renewable eugenol and α, ω-diols via a continuous overheating method, Polym. Chem. 6 (2015) 7138–7148, https://doi.org/10.1039/C5PY01075F.
[40] A.A. Omar, M.H.M. Hanafi, N.H. Razak, A. Ibrahim, N.A. Afwanisa'Ab Razak, Best-evidence review of bio-based plasticizer and the effects on the mechanical properties of PLA, Chem. Eng. Trans. 89 (2021) 241–246, https://doi.org/10.3303/CET2189041.
[41] E.F. Santos, R.V. Oliveira, Q.B. Reiznautt, D. Samios, S.M. Nachtigall, Sunflower-oil biodiesel-oligoesters/polylactide blends: plasticizing effect and ageing, Polym. Test. 39 (2014) 23–29. https://www.sciencedirect.com/science/article/abs/pii/S0142941814001561.
[42] J.R. Sarasua, R.E. Prud'homme, M. Wisniewski, A.Le Borgne, N. Spassky, Crystallization and melting behavior of polylactides, Macromolecules 31 (1998) 3895–3905, https://doi.org/10.1021/ma971545p.
[43] M. Pluta, A. Galeski, Crystalline and supermolecular structure of polylactide in relation to the crystallization method, J. Appl. Polym. Sci. 86 (2002) 1386–1395, https://doi.org/10.1002/app.11280.
[44] A. Magon, M. Pyda, Study of crystalline and amorphous phases of biodegradable poly(lactic acid) by advanced thermal analysis, Polymer 50 (2009) 3967–3973, https://doi.org/10.1016/j.polymer.2009.06.052.
[45] A. Hale, H.E. Bair, Polymer blends and block copolymers, in: E.A. Turi (Ed.), Thermal Characterization of Polymeric Materials, Academic Press, San Diego, 1997, pp. 745–886.
[46] Z. Li, P. Wei, Y. Yang, Y. Yan, D. Shi, Synthesis of a hyperbranched poly (phosphamide ester) oligomer and its high-effective flame retardancy and accelerated nucleation effect in polylactide composites, Polym. Degrad. Stab. 110 (2014) 104–112, https://doi.org/10.1016/j.polymdegradstab. 2014.08.024.
[47] N. Burgos, P. Fiori, A. Jiménez, D. Tolaguera, Synthesis and characterization of lactic acid oligomers: Evaluation of performance as poly (lactic acid) plasticizers, J. Polym. Environ. (2014) 227–235, https://doi.org/10.1007/s10924-013-0628-5.
[48] N. Ljungberg, B. Wesslen, Tributyl citrate oligomers as plasticizers for poly (lactic acid): thermo-mechanical film properties and aging, Polymer 44 (2003) 7679–7688, https://doi.org/10.1016/j.polymer.2003.09.055.
[49] J. Zhang, K. Tashiro, H. Tsuji, A.J. Domb, Disorder-to-order phase transition and multiple melting behavior of poly(l-lactide) investigated by simultaneous measurements of WAXD and DSC, Macromolecules 41 (2008) 1352–1357, https://doi.org/10.1021/ma0706071.
[50] X. Guo, J. Zhang, J. Huang, Poly(lactic acid)/polyoxymethylene blends: morphology, crystallization, rheology, and thermal mechanical properties, Polymer 69 (2015) 103–109, https://doi.org/10.1016/j.polymer.2015.05.050.
[51] H. Xiao, W. Lu, J.T. Yeh, Effect of plasticizer on the crystallization behavior of poly (lactic acid), J. Appl. Polym. Sci. 113 (2009) 112–121, https://doi.org/10.1002/app.29955.
[52] P. Pan, W. Kai, B. Zhu, T. Dong, Y. Inoue, Polymorphous crystallization and multiple melting behavior of poly(l-lactide): molecular weight dependence, Macromolecules 40 (2007) 6898–6905, https://doi.org/10.1021/ma071258d.
[53] J. Zhang, Y. Duan, H. Sato, H. Tsuji, I. Noda, S. Yan, Y. Ozaki, Crystal modifications and thermal behavior of poly(l-lactic acid) revealed by infrared spectroscopy, Macromolecules 38 (2005) 8012–8021, https://doi.org/10.1021/ma051232r.
[54] J. Hoffman, J. Lauritzen, Crystallization of bulk polymers with chain folding: theory of growth of lamellar spherulites, J. Res. Natl. Bur. Stand. 65 (1961) 297, https://doi.org/10.6028/jres.065A.035.